Journal of Engineering and Applied Sciences 13 (12): 4406-4413, 2018
ISSN: 1816-949X


# Enhanced Photocatalytic Degradation of Methyl Orange using Ag-Doped $TiO_2$ Photocatalyst

[1]Ying Pei Lim, [2]Ying Chin Lim, [3]Devagi Kanakaraju and [1]Huey Ling Tan
[1]Faculty of Chemical Engineering,
[2]Faculty of Applied Sciences, Universiti Teknologi MARA, 40450 Shah Alam, Selangor, Malaysia
[3]Faculty of Resource Science and Technology, Universiti Malaysia Sarawak, Sarawak, Malaysia

**Abstract:** In the present study, Ag-doped Titanium dioxide (Ag-$TiO_2$) photocatalyst was prepared by wet impregnation method. The effect of dopant concentration, incubation temperature and incubation time on the photocatalytic degradation of Methyl Orange (MO) in aqueous suspension under Ultra Violet (UV) light irradiation were studied systematically. The synthesized photocatalyst was characterized using XRD and SEM-EDX mapping. The characterization results confirmed that Ag was successfully doped into $TiO_2$ with anatase phase structure. The Ag-$TiO_2$ photocatalyst exhibited the highest dye removal of 85% efficiency with 5 wt.% dopant concentration when the incubation temperature and time were 70°C and 8 h, respectively. The kinetic study revealed that photocatalytic reaction follows Langmuir Hinshelwood (L-H) Model and pseudo-first order law with the highest regression coefficient of 0.992. Ag-$TiO_2$ was found to be an efficient photocatalyst showing enhanced photocatalytic activity for MO decolorization under UV irradiation.

**Key words:** Dye, titanium oxide, doping, photocatalyst, photodegradation, Ag-$TiO_2$

## INTRODUCTION

Dyes are used primarily in the production of consumer products including paints, textiles, cosmetics, plastics and papers. Dye containing waste waters are usually recalcitrant to degradation by the conventional biological treatments due to its high toxicity as these compounds are often hardly biodegradable or even biocides (Oller *et al*., 2011). The main issue is dyes contain a number of dangerous chemical substances such as dioxin, formaldehyde and heavy metals. These substances can potentially cause acute and chronic effects on the exposed living organisms and due to their stability, dyes remain in the environment for a long period of time. Besides, the presence of dyes on water surface prevents the sunlight from penetrating into the water and thus retards algae photosynthesis.

There are several decrement technologies including adsorption (Kyzas and Matis, 2015), microbial degradation (Casalatto *et al*., 2011) and advanced oxidation processes (Zuorro and Lavecchia, 2014) which have been proposed for removal of azo dyes from textile discharges. Photocatalysis, however, offers better solutions compared to the other technologies for the removal of azo dyes due to its ability to mineralize the pollutants completely. $TiO_2$ is feasible in terms of its inexpensiveness, non-toxicity and high redox potentials (Tan *et al*., 2017). Nevertheless, pure unmodified $TiO_2$ has several drawbacks including its wide band gap energy level 3.0~3.2 eV resulting in poor absorbance of visible light (Hou *et al*., 2009), low quantum efficiency derived from the high recombination rate of photo-induced electron-hole ($e^-/h^+$) pairs (Gou *et al*., 2017), rapid recombination rate of photo-generated electron-hole pairs and inefficient utilization of UV light (Zhao *et al*., 2016). In this regard, modification of $TiO_2$ surface by metal doping was proven to enhance its photocatalytic activity (Mohamed *et al*., 2013) through electrons trapping which can greatly increase the efficiency of charge separation and also prevent recombination of electron-hole pairs. Behnajady and Eskandarloo (2013) showed that Ag-doped $TiO_2$ by liquid impregnation method improved the photocatalytic performance in the degradation of AR88. Zuas and Budiman (2013) used co-precipitation method to dope 3 wt.% of Cu with $TiO_2$. 90% of Congo Red dye was decolorized over Cu-$TiO_2$ photocatalyst, compared to

**Corresponding Author:** Ying Pei Lim, Faculty of Chemical Engineering, Universiti Teknologi MARA, 40450 Shah Alam, Selangor, Malaysia

53% using pure $TiO_2$ (Lei *et al*., 2016). Lei *et al.* (2016) also showed better photocatalytic performance for the impregnated $Cu/TiO_2$ in the degradation of both decabromodiphenyl ether (BDE209) and Tetrabromodiphenyl ether (BDE47) when exposed to UV irradiation in an anoxic atmosphere. Besides, Wang *et al.* (2016) reported the degradation of salicylic acid over iodine and nitrogen co-doped $TiO_2$ photocatalyst. Presence of iodine increased the rate constant of the acid removal and 78.3% of total organic carbon was eliminated upon 180 min under visible light irradiation. Although, these studies aimed to improve $TiO_2$ activity by metal doping, investigation of the process parameters during metal-doped $TiO_2$ experiments is still lacking. Therefore, this study was carried out with the aim to synthesize nanostructured Ag-doped titania at different dopant concentration, incubation time and temperature by the wet impregnation method. The synthesized Ag-doped $TiO_2$ photocatalysts were characterized for their phase structures and surface morphologies and subsequently investigated for their photocatalytic activity. The photocatalytic activity of the synthesized samples was investigated to decolorize MO dye as the model compound in aqueous solution under UV irradiation.

## MATERIALS AND METHODS

**Chemicals and materials:** Commercial $TiO_2$ (reported surface area 10 $m^2/g$) was used as the starting material for the synthesis Ag-$TiO_2$ photocatalyst. Sodium hydroxide and silver nitrate were purchased from Merck all chemicals were used without further purification. Methyl Orange (MO) ($(CH_3)_2NC_6H_4NNC_6H_4SO_3Na$) with formula weight of 327 g/mol was obtained from Sigma Aldrich. All the reagents used were of analytical grade and solutions were prepared using distilled water.

**Preparation of Ag-$TiO_2$ photocatalyst:** The Ag-$TiO_2$ photocatalyst was prepared according to the procedures adopted by Lei *et al.* (2016) using wet impregnation method. The optimum concentration of Ag was firstly determined with varying Ag concentration between 5-20 wt.%. To prepare 5 wt.% $Ag/TiO_2$, 9.2126 g of $TiO_2$ was dispersed in 50 mL of distilled water. Under continuous stirring, 0.7874 g of silver nitrate was added to the diluted $TiO_2$ solution. The mixture was next incubated in a water bath for 2 h at 90°C. The product was then washed and calcined overnight in a furnace at 450° C. The aforesaid preparation steps were repeated by varying the incubation temperature between 25-70°C and incubation time of 1-24 h, respectively by using the optimum Ag concentration obtained. For comparison purposes, $TiO_2$ without dopant was prepared through the same method and calcined at 450°C.

**Characterization of Ag-$TiO_2$ photocatalyst:** It is important to characterize the calcined photocatalysts in order to determine their chemical and physical properties and relate these properties to their photocatalytic performance. The morphology of selected samples were characterized using a Field Emission Electron Microscope (FESEM) (Carl Zeiss SUPRA 40VP) and an Energy Dispersive X-ray (EDX) (Carl Zeiss SUPRA 40 VP). Meanwhile, the X-Ray Diffraction (XRD) (X'Pert Pro-MPD, PAN alytical) system was operated at 40 kV and 30 mA with a scanning range of $2\theta$ = 10-90° using Cu K$\alpha$ ($\lambda$ = 1.504Å) to determine the phases of the photocatalyst. The crystallite sizes were calculated with the Scherrer equation ($\Phi = K\lambda/\beta\cos\theta$) where $\Phi$ is the crystallite size, K is usually taken as 0.89, $\theta$ is the wavelength of the X-ray radiation (0.154 nm), $\beta$ is the Full Width at Half-maximum Intensity (FWHM) and $\theta$ is the diffraction angle of the 101 peak for anatase at $2\theta$ = 25.4°. Brunauer-Emmett-Teller (BET) was used to investigate the surface area of the photocatalyst. The sample was preheated at 200°C for 5 h and degassed under vacuum before measurements.

**Control study:** For adsorption study, the sample was conducted in the dark. In each test, 1 g of Ag-$TiO_2$ photocatalyst sample was added into a 200 mL of 10 ppm MO dye to form suspensions into a glass cell with dimension 150×100×100 mm (L×B×H) and aerated as shown in Fig. 1. An aquarium pump model NS 7200 was used as the aeration source. The degradation efficiency of MO was determined at specific time interval until saturation time was achieved (180 min). For photolysis study, similar experimental conditions with adsorption study were adopted under UV irradiation in the absence of $TiO_2$ photocatalyst. The absorbance was measured by using UV-Vis spectrometer (Shimadzu, UV-210A) at 476 nm to detect the changes in MO concentration. A linear calibration of absorption vs. concentration was obtained. Subsequently, degradation efficiency was determined using the following Eq. 1.

$$\xi = \frac{C_o - C_t}{C_o} \times 100\% \quad (1)$$

Where:

$\xi$ = MO degradation efficiency
$C_o$ = Initial concentration of MO
$C_t$ = Final concentration of MO

**Photocatalytic degradation of Methyl Orange (MO):** The photocatalytic degradation of MO was carried out in a photoreactor equipped with 15 W UV lamp at the height of 5 cm from the surface of MO solution. The solution was magnetically stirred for 15 min in the dark to reach adsorption-desorption equilibrium with Ag-$TiO_2$ photocatalyst before the lamp was turned on to start the photo reaction. The 3 mL of sample solution was with drawn using syringe at a fixed time interval of 15 min and the collected sample was filtered through a 0.5 μm filter to obtain clear solution prior to analysis. The photocatalytic degradation experiment was repeated using the bare $TiO_2$.

## RESULTS AND DISCUSSION

**Characterization of Ag-$TiO_2$ Photocatalyst:** Figure 1 and 2 shows the XRD pattern of bare $TiO_2$ and Ag-$TiO_2$ photocatalyst. Bare $TiO_2$ matches JCPDS 00-021-1272 which indicates the anatase structure. There is no trace of rutile and brookite phases which is favorable as anatase has better photocatalytic activity than other phases. The XRD result revealed at $2\theta$ = 25.28, 37.8, 48.05, 53.89, 55.06 and 62.69° corresponding to crystal planes of (101), (004), (200), (105), (211) and (204) (JCPDS 21-1272). Mogal *et al.* (2014) also obtained the anatase structure of $TiO_2$ at the same peaks corresponding to crystal planes of (200) and (220) (JCPDS 01-1164) (Mogal *et al.*, 2014). After the addition of Ag, it can be seen that most of the $2\theta$ peak positions of the major diffraction pattern in all samples show no shifting, having similar values of bare $TiO_2$. The diffraction peak at 44.1° of metallic Ag was detected in Fig. 2, however, at 10 wt.% Ag and above. It could be probably Ag is situated in the bulk (inside the $TiO_2$ crystals) at lower concentrations. The result is in agreement with the research work by Melian *et al.* (2012), Mohamed and Al-Sharif (2013). In addition, another additional peak was also spotted at 64.2°. The intensity of the Ag peaks increases gradually as the weight percentage of Ag increases. The presence of Ag phase does not change the crystalline structure of the $TiO_2$ substrate. This may indicate that Ag is formed on the crystal borders and on the surface of the $TiO_2$.

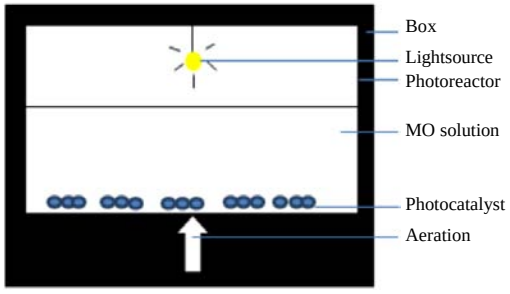


Fig. 1: Schematic diagram of photocatalytic degradation of MO

The crystallite size for Ag-$TiO_2$ prepared at various Ag loading was estimated from Scherrer equation and is tabulated in Table 1. From Table 1, the crystallite size for bare $TiO_2$ is approximately 94 nm and the size generally

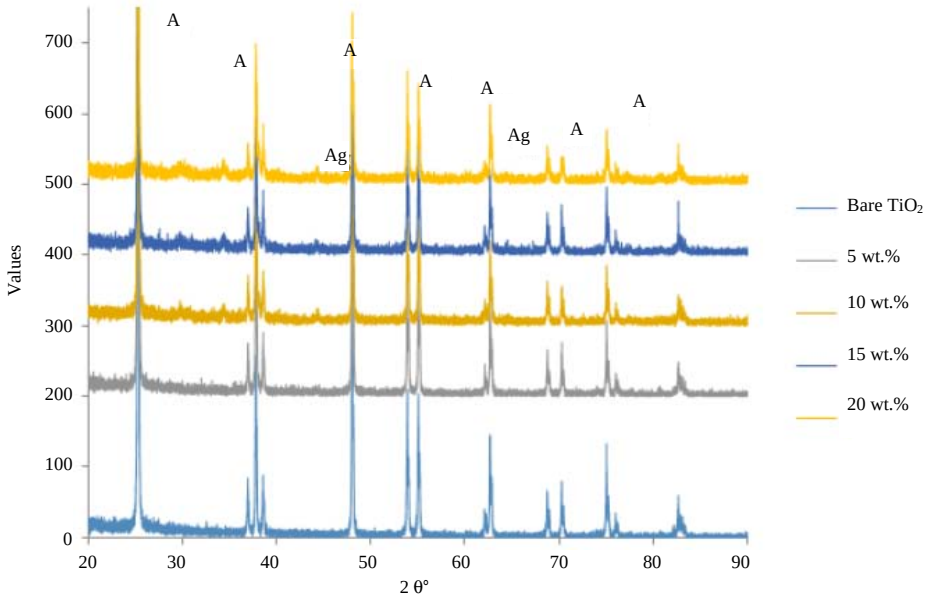


Fig. 2: XRD pattern of Ag/$TiO_2$ at different Ag concentration (Ag = Silver, A = Anatase)

Table 1: Crystallite size for $TiO_2$ and $AgTiO_2$ prepared at various concentrations

| Sample | Crystallite size (nm) |
|---|---|
| Bare $TiO_2$ | 93.9 |
| 5 wt.% $AgTiO_2$ | 57.4 |
| 10 wt.% $AgTiO_2$ | 66.8 |
| 15 wt.% $AgTiO_2$ | 86.1 |
| 20 wt.% $AgTiO_2$ | 73.8 |

decreases to 57-86 nm upon incorporation of Ag particles. However, the crystallite size for $AgTiO_2$ increases with increasing Ag concentration from 5-20 wt.%.

On the other hand, the correlation between elemental composition and morphological changes of particles can be identified by EDX, since, the composition is very sensitive for the application. Figure 3 shows the EDX spectra of bare $TiO_2$ and Ag-$TiO_2$ photocatalyst. From Figure 3a, Ti peaks were observed at 0.45 and 4.51 keV while the O peak was detected at 0.52 V. These peaks were originated from $TiO_2$. Meanwhile, the Ag peak was successfully identified at 2.9 and 3.15 keV as shown in Fig. 3b. Even though, the peaks of Ag are insignificant owing to its content in $TiO_2$ matrix, they indicate the Ag present in the photocatalyst and thus, support XRD findings. The presence of Ag originated from the Ag precursor ($AgNO_3$) used in the preparation of Ag-$TiO_2$ photocatalyst. The atomic percentage of Ti, O and Ag in Ag-$TiO_2$ were 33.07, 66.58 and 0.34 wt.%, respectively. Mapping analysis was performed to observe the dispersion of Ag on $TiO_2$ surface. From Fig. 4, the EDX mappings show the uniform dispersion of Ag onto the surface of $TiO_2$ and present in the form of metal oxides (Ag oxides).

FESEM analysis was performed in order to observe the changes of the $TiO_2$ morphological structure when Ag was incorporated. Figure 5 shows the FESEM images of bare $TiO_2$ and Ag-$TiO_2$. Bare $TiO_2$ comprises of spherical and square-like shape with irregular sizes. It can be seen that slightly agglomeration occurred in the certain spot. There were no distinct changes on the shape of $TiO_2$ after Ag was impregnated. However, it can be observed that the color changed from white to grey upon impregnation. The changes in the color proved that Ag was successfully impregnated on $TiO_2$ surface in agreement with the existence of Ag peaks in EDX spectra. TEM analysis was performed to observe the Ag-$TiO_2$ particles at higher magnification (50 kX) and the TEM micrograph is shown in Fig. 6. Apparently, spherical-like shaped $TiO_2$ particles could be seen and this observation is tally with the one observed using FESEM. However, a close inspection of the TEM image showed that tiny round particles was observed to deposit on the surface of the

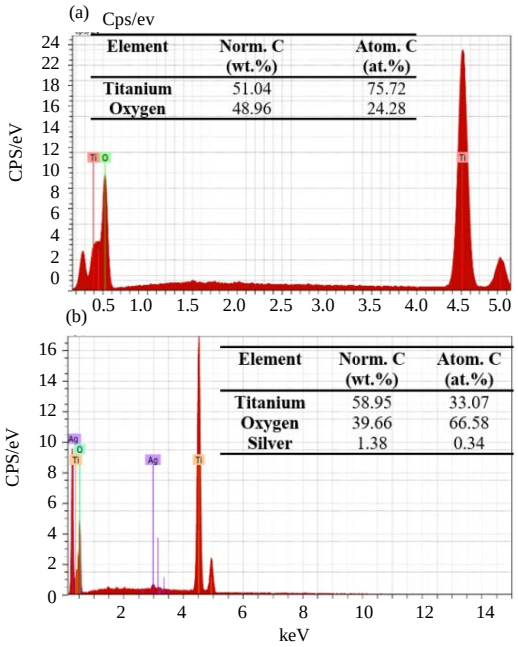


Fig. 3: EDX spectra of: a) Bare $TiO_2$ and b) Ag-$TiO_2$ with 2 h of incubation time

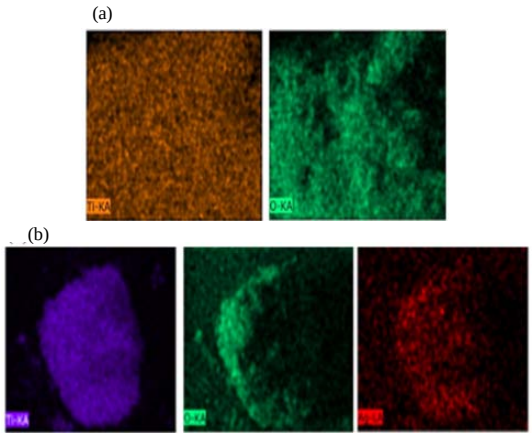


Fig. 4: EDX mappings of: a) Bare $TiO_2$ and b) Ag-$TiO_2$

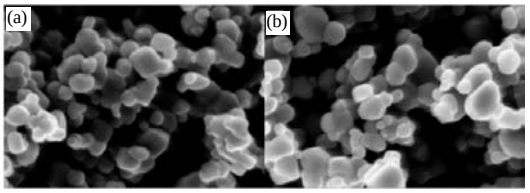


Fig. 5: FESEM images of: a) Bare $TiO_2$ and b) Ag-$TiO_2$ photocatalyst

$TiO_2$ particles and it is presumably to be the Ag particles. Nevertheless, the tiny particles were not distributed homogenously on the surface of $TiO_2$

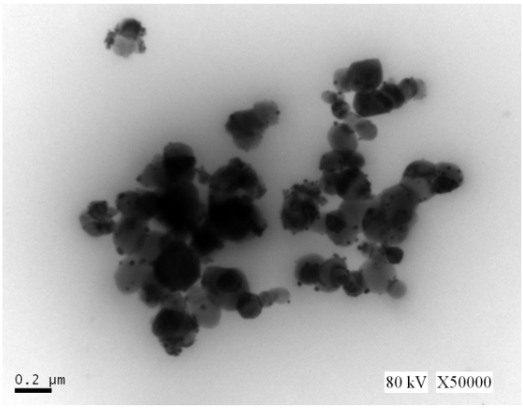


Fig. 6: TEM images of Ag-$TiO_2$ photocatalyst

In order to get better photocatalytic activity, high surface area of the catalyst is often desired. The BET surface area of bare $TiO_2$ was found to be 9.71 $m^2$/g which is close to the value reported in the technical datasheet (10 $m^2$/g). It was observed that when Ag was introduced, the surface area decreased slightly to 9.32 $m^2$/g. Surface area decreased with the increasing Ag loading in Ag-$TiO_2$ photocatalyst. This could be due to partial pore obstruction caused by the deposition of Ag aggregates on the $TiO_2$ surface (Sakthivel *et al*., 2004, Zhao *et al*., 2011).

**Photocatalytic performance of Ag-$TiO_2$ photocatalyst:** The photocatalytic performance of Ag-$TiO_2$ photocatalyst for the removal of MO was studied based on the reaction kinetics at different parameters.

**Effect of Ag concentration:** From Fig. 7, it can be clearly seen that the optimum metal loading of Ag-$TiO_2$ is at 5 wt.% with MO removal efficiency of 68.2%. Compare to bare $TiO_2$, Ag-$TiO_2$ photocatalyst show higher removal efficiency up to Ag loading of 15 wt.% and then decreases. At 5 wt.% Ag, the metallic Ag particles deposited on $TiO_2$ surfaces acted as electron scavengers and contributed to the decrease of electron-hole recombination in $TiO_2$. In contrast in high Ag content, it has been reported that the probability for the hole capture is increased by a large number of negatively charged Ag particles on $TiO_2$ which reduces the efficiency of charge separation (Hosseini *et al*., 2011). Moreover, the dopants could behave as electron/hole recombination center thus lowering the performance of photocatalytic activity. Melian *et al*. (2012) also found that excess in Ag loaded into $TiO_2$ leads to low photocatalytic activity. A similar finding was also reported by Vamathevan *et al*. (2002) who used sucrose as model compound in his study.

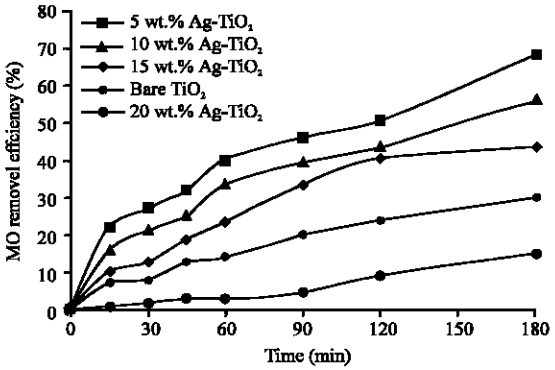


Fig. 7: MO removal efficiency with different Ag concentration

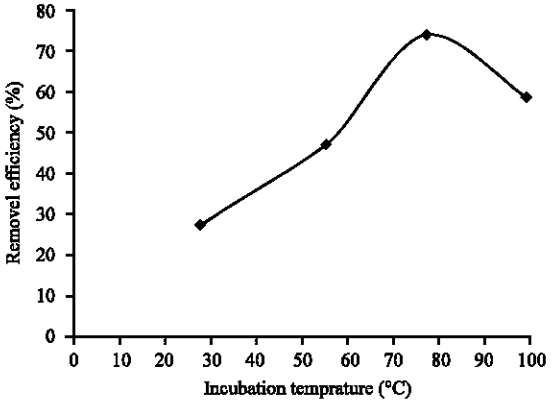


Fig. 8: Comparison of removal efficiency of MO at different incubation temperature

**Effect of incubation temperature:** The condition of preparation of Ag-$TiO_2$ also influences the reaction of the catalyst. Figure 8 illustrates the percentage removal of MO solution at different incubation temperature. After 3 h of degradation process, the incubation temperature at 25°C showed the lowest removal efficiency of MO which was 27.4% while the highest MO removal efficiency was at 70°C with 73.5%. The incubation temperature of 70°C could have changed the surface properties of the Ag-$TiO_2$ photocatalyst which is in agreement with BET surface area analyses. Ag-$TiO_2$ at 5 wt.% Ag loading has the largest BET surface area among all modified $TiO_2$ samples (9.53 $m^2$/g). The larger surface area as well as the increase in pore volumes provides a more interfacial area for the reaction to occur, thus, increasing the photo-degradation activity of MO.

**Effect of incubation time:** Based on Fig. 9, the degradation rate of MO was improved with increasing incubation time between 1-8 h and then decreased thereafter. The highest MO removal obtained was 84.9% at 8 h of incubation time.

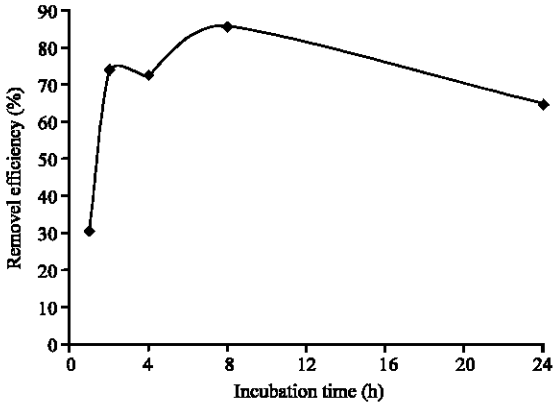


Fig. 9: Removal effiency of MO at different incubation time

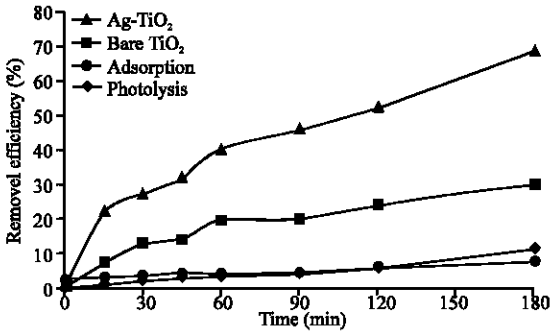


Fig. 10: Comparison of MO removal efficiency between Ag-$TiO_2$ and control tests

Prolonging the incubation time promoted the growth of photocatalyst particles, thus, lead to agglomeration (Reli *et al*., 2002). As a result, this would reduce the surface area of photocatalyst as well as its photocatalytic activity due to weakening interaction between Ag-$TiO_2$ photocatalyst (Cheng *et al*., 2007).

Figure 10 compares the optimum performance of Ag-$TiO_2$ photocatalyst on the removal of MO with control experiments. The control experiments were conducted under the same conditions for MO photo-degradation test except for photolysis which was carried out without the presence of catalyst and without the presence of UV light source for adsorption. The order of degradation of MO was as follows, Ag-$TiO_2$ (UV)>bare $TiO_2$ (UV)>photolysis>adsorption. Photolysis and adsorption led to the little removal of MO. Thus, it can be established that the photocatalytic performance can be enhanced by reacting the photocatalyst samples under UV light irradiation as it can excite more electrons and holes in $TiO_2$.

**Kinetics study of photodegradation of MO:** The photocatalytic degradation of MO fitted well with the pseudo-first-order kinetic model for both bare $TiO_2$ and Ag-$TiO_2$. The reaction rate is written in the form of:

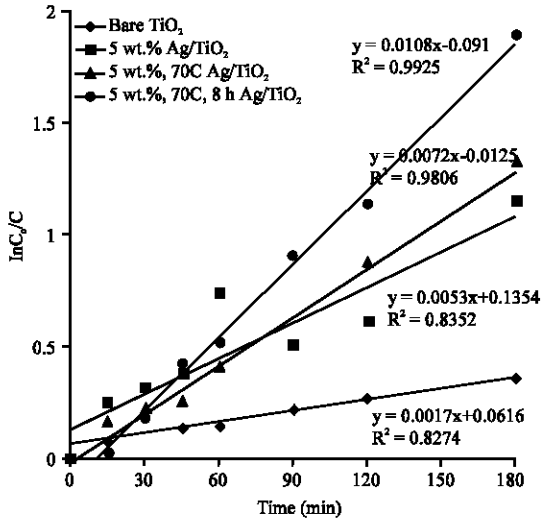


Fig. 11: Kinetics of photodegradation of MO at optimum parameters

$$r = \frac{-dc}{dt} = kC \quad (2)$$

Where:

k = The pseudo-first order reaction rate coefficient
C = The concentration of MO

The integration of the expression with $C = C_0$ at $t = 0$ gives:

$$\int_{C_0}^{C} \frac{-dC}{C} = k \int dt \quad (3)$$

$$-(\ln C - \ln C_0) = kt \quad (4)$$

$$\ln \frac{C_0}{C} = kt \quad (5)$$

The half-life of Ag-$TiO_2$ photocatalyst which was described as the time taken for the amount of photocatalyst to decrease by half can be obtained from the reaction rate coefficients. It was calculated using the following Eq. 6:

$$t_{1/2} = \frac{\ln 2}{k} \quad (6)$$

Plotting the natural logarithm of the ratio of MO initial concentration and the concentration after photocatalytic degradation ($\ln C_0/C$) versus irradiation time (min.) yields a linear relationship as shown in Fig. 11. The rate constants, k are obtained from the slope of the graphs.

Table 2: Rate coefficients, $R^2$ values and half-lives at different parameter

| Parameters | k ($min^{-1}$) | $R^2$ | Half-life (min) |
|---|---|---|---|
| Concentration (ppm) | $5.3\times10^{-3}$ | 0.835 | 130.77 |
| Incubation temperature (°C) | $7.2\times10^{-3}$ | 0.981 | 96.25 |
| Incubation time (h) | $1.08\times10^{-2}$ | 0.992 | 64.29 |

Table 2 summarizes the reaction rate coefficients obtained from the slope of the graphs with its respective R-squared values ($R^2$) and the half-lives of the photocatalyst. From Table 2, the degradation of MO using Ag-$TiO_2$ photocatalyst prepared at 5 wt.% of Ag, 70°C of incubation temperature and 8 h of incubation time demonstrated the highest rate constant of $1.08\times10^{-2}$ $min^{-1}$ and $R^2$ value of 0.992. The half-life was 64.29 min.

## CONCLUSION

The objectives of the study were to prepare hybrid Ag-$TiO_2$ photocatalyst by wet impregnation method using different Ag concentration, incubation temperature and incubation time as well as to investigate the photocatalytic activity on the degradation of MO. The prepared photocatalyst was characterized using XRD, BET, EDX and FESEM analyses. The XRD analysis illustrated the anatase structure of $TiO_2$. The EDX spectra showed the composition of Ag on $TiO_2$ surface while the mappings showed the presence of Ag with uniform distribution on $TiO_2$ surface. The FESEM images showed the spherical and square-like shape of $TiO_2$. The colour also changed from grey to white when Ag was incorporated. This study also proved that Ag-$TiO_2$ photocatalyst has better photocatalytic performance over bare $TiO_2$, photolysis and also adsorption in the removal of MO dye. The photocatalyst prepared using 5 wt.% of Ag at 70°C and 8 h of incubation temperature and time showed an optimum result in which the photocatalyst was able to remove 84.94% of MO with in 3 h. The reaction kinetics also showed that the rate coefficient of Ag-$TiO_2$ was $1.08\times10^{-2}$ $min^{-1}$ and the half-life obtained was 64.29 min. The study suggested that Ag-$TiO_2$ is a promising photocatalyst for the degradation of organic pollutants under UV irradiation.

## ACKNOWLEDGEMENTS

The reseracher would like to acknowledge Faculty of Chemical Engineering and Faculty of Applied Sciences, Universiti Teknologi MARA for the facilities provided. This study was financially supported by Universiti Teknologi MARA, through the LESTARI Grant (600-IRMI/DANA KCM 5/3/LESTARI (192/2017).

## REFERENCES

Behnajady, M.A. and H. Eskandarloo, 2013. Characterization and photocatalytic activity of Ag-Cu/$TiO_2$ nanoparticles prepared by sol-gel method. J. Nanosci. Nanotechnol., 13: 548-553.

Caselatto, A.M.F., J.F. Ferreira, E.B. Tambourgi, R. Moraes and E. Silveira, 2011. Biodegradation of textile azo dyes by Shewanella putrefaciens (CCT 1967). Chem. Eng., 24: 871-876.

Cheng, Y., S.U.N. Hongqi, J. Wanqin and X.U. Nanping, 2007. Effect of preparation conditions on visible photocatalytic activity of titania synthesized by solution combustion method. Chin. J. Chem. Eng., 15: 178-183.

Gou, J., Q. Ma, X. Deng, Y. Cui and H. Zhang *et al*., 2017. Fabrication of $Ag_2O$/$TiO_2$-Zeolite composite and its enhanced solar light photocatalytic performance and mechanism for degradation of norfloxacin. Chem. Eng. J., 308: 818-826.

Hosseini, M.G., M. Shokri, M. Khosravi, R. Najjar and M. Darbandi, 2011. Photodegradation of an azo dye by silver-doped nano-particulate titanium dioxide. Toxicol. Environ. Chem., 93: 1591-1601.

Hou, X.G., M.D. Huang, X.L. Wu and A.D. Liu, 2009. Preparation and studies of photocatalytic silver-loaded $TiO_2$ films by hybrid sol-gel method. Chem. Eng. J., 146: 42-48.

Kyzas, G.Z. and K.A. Matis, 2015. Nanoadsorbents for pollutants removal: A review. J. Mol. Liquids, 203: 159-168.

Lei, M., N. Wang, L. Zhu, Q. Zhou and G. Nie *et al*., 2016. Photocatalytic reductive degradation of polybrominated diphenyl ethers on CuO/$TiO_2$ nanocomposites: A mechanism based on the switching of photocatalytic reduction potential being controlled by the valence state of copper. Appl. Catal. B Environ., 182: 414-423.

Melian, E.P., O.G. Diaz, J.D. Rodriguez, G. Colon and J.A. Navio *et al*., 2012. Effect of deposition of silver on structural characteristics and photoactivity of $TiO_2$-based photocatalysts. Appl. Catal. B Environ., 127: 112-120.

Mogal, S.I., V.G. Gandhi, M. Mishra, S. Tripathi and T. Shripathi *et al*., 2014. Single-step synthesis of silver-doped titanium dioxide: Influence of silver on structural, textural and photocatalytic properties. Ind. Eng. Chem. Res., 53: 5749-5758.

Mohamed, M.M. and M.S. Al-Sharif, 2013. Visible light assisted reduction of 4-nitrophenol to 4-aminophenol on Ag/$TiO_2$ photocatalysts synthesized by hybrid templates. Appl. Catal. B Environ., 142: 432-441.

Oller, I., S. Malato and J.A. Sanchez-Perez, 2011. Combination of advanced oxidation processes and biological treatments for wastewater decontamination-a review. Sci. Total Environ., 409: 4141-4166.

Reli, M., K. Koci, V. Matejka, P. Kovar and L. Obalova, 2012. Effect of calcination temperature and calcination time on the kaolinite/$TIO_2$ composite for photocatalytic reduction of $CO_2$/Vliv kalcinacni teploty a doby kalcinace na kompozit kaolinit/$TIO_2$ pro fotokatalytickou redukci $CO_2$. GeoSci. Eng., 58: 10-22.

Sakthivel, S., M.V. Shankar, M. Palanichamy, B. Arabindoo and D.W. Bahnemann *et al*., 2004. Enhancement of photocatalytic activity by metal deposition: Characterisation and photonic efficiency of Pt, Au and Pd deposited on $TiO_2$ catalyst. Water Res., 38: 3001-3008.

Tan, L.L., W.J. Ong, S.P. Chai and A.R. Mohamed, 2017. Photocatalytic reduction of $CO_2$ with $H_2O$ over graphene oxide-supported oxygen-rich $TiO_2$ hybrid photocatalyst under visible light irradiation: Process and kinetic studies. Chem. Eng. J., 308: 248-255.

Vamathevan, V., R. Amal, D. Beydoun, G. Low and S. McEvoy, 2002. Photocatalytic oxidation of organics in water using pure and silver-modified titanium dioxide particles. J. Photochem. Photobiol. A Chem., 148: 233-245.

Wang, X., J. Song, J. Huang, J. Zhang and X. Wang *et al*., 2016. Activated carbon-based magnetic $TiO_2$ photocatalyst codoped with iodine and nitrogen for organic pollution degradation. Appl. Surf. Sci., 390: 190-201.

Zhao, W., L. Feng, R. Yang, J. Zheng and X. Li, 2011. Synthesis, characterization and photocatalytic properties of Ag modified hollow $SiO_2$/$TiO_2$ hybrid microspheres. Appl. Catal. B Environ., 103: 181-189.

Zhao, W., Z. Zhang, J. Zhang, H. Wu and L. Xi *et al*., 2016. Synthesis of Ag/$TiO_2$/graphene and its photocatalytic properties under visible light. Mater. Lett., 171: 182-186.

Zuas, O. and H. Budiman, 2013. Synthesis of nanostructured copper-doped titania and its properties. NanoMicro Lett., 5: 26-33.

Zuorro, A. and R. Lavecchia, 2014. Evaluation of UV/$H_2O_2$ advanced oxidation process (AOP) for the degradation of diazo dye Reactive Green 19 in aqueous solution. Desalin. Water Treat., 52: 1571-1577.